Preparation, Structure, and Imaging of Luminescent SiO2 Nanoparticles by Covalently Grafting Surfactant-Encapsulated Europium-Substituted Polyoxometalates

ARTICLE *in* LANGMUIR · NOVEMBER 2010

Impact Factor: 4.46 · DOI: 10.1021/la103463w · Source: PubMed

Langmuir
Article
pubs.acs.org/Langmuir

Preparation, Structure, and Imaging of Luminescent SiO_2 Nanoparticles by Covalently Grafting Surfactant-Encapsulated Europium-Substituted Polyoxometalates

Yuanyuan Zhao, Yue Li, Wen Li, Yuqing Wu, and Lixin Wu*

State Key Laboratory for Supramolecular Structure and Materials, College of Chemistry, Jilin University, Changchun 130012, China

Received August 31, 2010. Revised Manuscript Received October 20, 2010

A novel route to the preparation of luminescent silica nanoparticles and coloration for living cells was demonstrated in this article. A europium-substituted polyoxometalate was encapsulated by a hydroxyl-group-terminated double-chain quaternary ammonium cation through an ion replacement process, yielding an organic−inorganic complex with core−shell structure bearing hydroxyl groups located at the periphery. The introduction of −OH groups not only increased the solubility of the complex in polar solvents but also caused it to embed into the inner matrix of silica nanoparticles covalently and be well-dispersed through an in situ sol−gel reaction with tetraethyl orthosilicate. Elemental analysis and spectral characterization confirmed the formation of prepared complexes with the anticipated chemical composition. Scanning and transmission electron microscopy images illustrated the size change of luminescent nanoparticles with smooth surfaces and well-dispersed polyoxometalate complexes inside of the silica matrix. X-ray photonic spectra and ξ-potential measurements revealed the chemical association between the silica matrix and the complex. Luminescent spectral characterization indicated the well-retained photophysical property of Eu-substituted polyoxometalate in silica nanoparticles. The surface amino-modified silica nanoparticles were applied to cell coloration, and the dyed Hella cells were observed through laser confocal fluorescence microscopy.

Introduction

Polyoxometalates (POMs), as a class of inorganic metal oxide clusters, exhibit extensive functional properties, such as rich and interesting magnetic, electronic, medical, photochromic, electrochromic, and especially luminescence properties.[1] Because of the uniform sizes in one to several nanometers, various topologies, multinegative charges, and dispersibility in solution, POMs also become intriguing building blocks in the fabrication of functional nanomaterials.[2] However, the practical POM-based materials or devices are quite limited because of their inherent limitations, such as a narrow pH stabilizing range and the poor processability of pure POMs that exist in the crystalline state or powdered materials. Therefore, developing a suitable method to protect and utilize POMs becomes significant for creating the applicable potentials. Several routes have been developed to introduce POMs into inorganic, organic, and polymer matrices,[3] among which is a facile approach to the replacement of the charge-balancing counterions of the inorganic clusters with different functional-group-terminated cationic organic molecules.[4−6] The formed surfactant-encapsulated POMs (SEPs) through such a step thus become no longer soluble in water but soluble in organic media. Importantly, the modified POMs can be easily organized into soft materials such as liquid crystals, patterned surfaces, inverse bilayer vesicles, and polymers[6] through the suitable selection of surfactants and POMs. In addition, by exchanging the terminal group of the surfactant with a reactive group, we successfully prepared a novel luminescent polymer and bulk silica through a sol−gel process.[6] Perceptibly, the advanced features introducing SEPs into polymer and silica through chemical bonds rather than direct physical blending of naked POMs are the following: (1) Proper surface modification can make POMs easier to disperse in the reaction system, thus increasing the miscibility with different matrices. (2) Chemical grafting of SEPs rather than incorporating naked POMs into organic and inorganic matrixes can preserve the cluster stability to a much greater extent. (3) Copolymerization can promote the nanoscale dispersion of SEPs and the homogeneity with carriers. (4) Because of the grafting groups on the surface, SEPs can serve as cross-linking agents to enhance the intrinsic properties of carriers.

Silica nanoparticles possess a variety of important features, such as biocompatibility, easy modification, chemical stability, and porosity, and have been applied as functional materials in photonic crystals, biological labeling, template preparation, catalyst carriers, and flow visualization probes.[7] To utilize these properties, the functionalization of silica nanoparticles has been extensively studied. These hybrid silica materials that can be simply modified and doped with luminescent and magnetic inorganic nanoparticles, even organic dyes, have

*To whom correspondence should be addressed. E-mail: wulx@jlu.edu.cn.

(1) (a) Hill, C. L. *Chem. Rev.* **1998**, *98*, 1–396.(b) Pope, M. T.; Müller, A. *Polyoxometalate Chemistry: From Topology via Self-Assembly to Application*; Kluwer: Dordrecht, The Netherlands, 2001.

(2) (a) Müller, A.; Kögerler, P.; Dress, A. W. M. *Coord. Chem. Rev.* **2001**, *222*, 193–218. (b) Long, D. L.; Burkholder, D. E.; Cronin, L. *Chem. Soc. Rev.* **2007**, *36*, 105–121. (c) Geletii, Y. V.; Botar, B.; Kögerler, P.; Hilleshiem, D. A.; Musaev, D. G.; Hill, C. L. *Angew. Chem., Int. Ed.* **2008**, *47*, 3896–3899.

(3) (a) Song, Y. F.; McMillan, N.; Long, D. L.; Kane, S.; Malm, J.; Riehle, M. O.; Pradeep, C. P.; Gadegaard, N.; Cronin, L. *J. Am. Chem. Soc.* **2009**, *131*, 1340–1341. (b) Pradeep, C. P.; Misdrahi, M. F.; Li, F. Y.; Zhang, J.; Xu, L.; Long, D. L.; Liu, T. B.; Cronin, L. *Angew. Chem., Int. Ed.* **2009**, *48*, 8309–8313. (c) Piedra-Garza, L. F.; Dickman, M. H.; Moldovan, O.; Breunig, H. J.; Kortz, U. *Inorg. Chem.* **2009**, *48*, 411–413. (d) Gao, G. G.; Xu., L.; Qu, X. S.; Liu, H.; Yang, Y. Y. *Inorg. Chem.* **2008**, *47*, 3402–3407. (e) Qi, W.; Wu, L. X. *Polym. Int.* **2009**, *58*, 1217–1225.

(4) (a) Kurth, D. G.; Lehmann, P.; Volkmer, D.; Cölfen, H.; Koop, M. J.; Müller, A.; Du Chesne, A. *Chem.−Eur. J.* **2000**, *6*, 385–393. (b) Nyman, M.; Rodriguez, M. A.; Anderson, T. M.; Ingersoll, D. *Cryst. Growth Des.* **2009**, *9*, 3590–3597.

(5) (a) Li, H. L.; Sun, H.; Qi, W.; Xu, M.; Wu, L. X. *Angew. Chem., Int. Ed.* **2007**, *46*, 1300–1303. (b) Yan, Y.; Li, B.; Li, W.; Li, H. L.; Wu, L. X. *Soft Mater.* **2009**, *5*, 4047–4053.

(6) (a) Qi, W.; Li, H. L.; Wu, L. X. *Adv. Mater.* **2007**, *19*, 1983–1987. (b) Li, H. L.; Qi, W.; Li, W.; Sun, H.; Bu, W. F.; Wu, L. X. *Adv. Mater.* **2005**, *17*, 2688–2692.

(7) Bergna, H. E.; Roberts, W. O. *Colloidal Silica Fundamentals and Applications*; CRC Press: Boca Raton, FL, 2006.

Scheme 1. Schematic Drawing of the Preparation and Structure of the SEP-1 Complex and SEP-1-Doped Silica Nanoparticles through a Sol−Gel Reaction

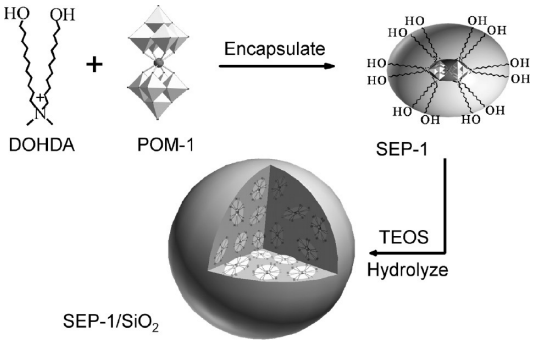

been exploited.[8] By mixing with amino acids, europium-substituted POMs have been successfully doped into silica particles and their photoluminescence has been confirmed by surviving for a number of days in water.[9a] However, in many cases, it is difficult to avoid the aggregation of embedded components when a high doping content is required.[9] Normally, multidoping and even dispersion are important in applicable materials for the promotion of catalytic efficiency and the luminescent stability of POMs.

To introduce POMs into silica nanoparticles in a more controllable way, in this article we describe a straightforward approach to the preparation of monodisperse, Eu-substituted POM-doped silica nanoparticles with highly luminescent stability, as represented in Scheme 1. Hydroxyl-group-terminated surfactant di(11-hydroxyundecyl)dimethylammonium bromide (DOHDA) was prepared and applied to the encapsulation of luminescent $Na_9EuW_{10}O_{36}$ (POM-1). The grafted 12 hydroxyl groups on the outside surface of the complex can make the obtained SEP-1 easily dissolve in the mixture of ethanol and water and react with siloxane agents, leading to hybrid silica nanoparticles (SEP-1/SiO_2) with SEP-1 chemically binding to the silica matrix uniformly. Besides acting as a luminescent dyeing agent, because of the property of POM-1,[10] the present strategy for SEP-doped silica nanoparticles has four advantages: (1) A general method is built to incorporate POMs, especially for pH-sensitive and unstable POMs, into silica nanoparticles. (2) The main properties of POMs, such as luminescence, are well protected during the preparation of hybrid silica nanoparticles. (3) The embedded POMs in silica nanoparticles are located in a hydrophobic microenvironment. (4) The leakage of POMs from the carrier silica matrix is effectively avoided.

Experimental Section

Chemicals. Dimethylamine, tetraethyl orthosilicate (TEOS), aminopropyltriethoxy silane (APS), and ammonia (28%) were purchased from Beijing Chemical Reagent Company. 11-Bromoundecanol with a purity of 97% was a product of Sigma-Aldrich. Except for TEOS being redistilled under reduced pressure just before use, all of the chemicals were used without any further purification. High-purity ethanol and ultrapure water (18.2 MΩ) purified from a Milli-Q Water system were used throughout the experiments.

Preparation of POM-1, DOHDA, and SEP-1. POM-1 was synthesized according to a published procedure and checked by single-crystal structure analysis.[11] DOHDA and SEP-1 were synthesized according to the exact description reported in the literature.[6a] ^{1}H NMR ($CDCl_3$) of DOHDA: δ 1.28 (m, 14H), 1.47 (m, 2H), 1.56 (m, 2H), 2.25 (s, 6H), 2.28 (t, 2H) and 3.64 (t, 2H). FT-IR (KBr) of SEP-1 (vibrations of DOHDA): 3368 (ν_s, O−H) and 3032 (ν_{as}, O−H), 2921 (ν_{as}, CH_2), 2850 (ν_s, CH_2), 1647 (δ, O−H), 1467 (δ, CH_2), 1056 cm^{-1} (ν_s C−O). FT-IR (KBr) of SEP-1 (vibrations of POM-1): 935 (ν_{as}, W−O_d), 840 (ν_{as}, W−O_c−W), and 782 cm^{-1} (ν_{as}, W−O_c−W).[6,12] Anal. Calcd [$(DOHDA)_6H_3EuW_{10}O_{36}\cdot 4H_2O$, 4769.5] (%): C, 34.86; H, 6.56; N, 1.69. Found: C, 35.45; H, 6.81; N, 1.52.

Preparation of SEP-1/SiO_2 Nanoparticles. In a typical procedure, to 50 mL of a 98% ethanol aqueous solution with 0.32 mg/mL SEP-1 was added 1.7 mL of TEOS and 2 mL of ammonia. After the solution was gently stirred for ca. 3 h at room temperature, light-blue scattering appeared and another 1.1 mL of TEOS was slowly added dropwise. After another 6 h of stirring, the reaction solution was centrifuged at 13 000 rpm for 15 min and then washed three times with water. The supernatant was collected and concentrated for further characterization. The obtained S4 product precipitate was then dispersed in 50 mL of water through sonication for further spectral, TEM, and XPS measurements. Through the same procedures, all SEP-1/SiO_2 samples, with SEP-1 doping concentrations at 0.00, 0.04, 0.08, 0.20, 0.32, 0.84, and 1.20 mg/mL (corresponding to mass percentages of 0, 0.3, 0.5, 1.3, 2.1, 5.3, and 7.4, respectively), were prepared and named S0, S1, S2, S3, S4, S5, and S6, respectively. Because of the small sizes of S5 and S6, we cannot obtain the precipitates through simple centrifugation. As a replacement procedure, the products were diluted with water and encountered repeated treatment with a rotatory evaporator under reduced pressure almost to dryness.

Preparation of −NH_2-Modified SEP-1/SiO_2 and Labeling of Hela Cells. In a typical procedure, 32 mg of SEP-1/SiO_2 (S5) was dispersed in 50 mL of ethanol under sonication, and then 2 mL of ammonia and 20 μL of APS were added under mechanical agitation. After 24 h of stirring, the solution was centrifuged at 18 000 rpm for 30 min at 4 °C. The obtained precipitate was washed with water three times, yielding surface amino-modified hybrid silica nanopariticle SEP-1/SiO_2@NH_2. Hela cells were cultured in Dulbecco's modified Eagle's medium (DMEM, Sigma) containing 10% fetal bovine serum (FBS, Gibco) and 1% antibiotic-antimycotic (Gibco) at 37 °C in a CO_2/air (5/95 volume ratio) incubater. The cells were plated into six well plates for 24 h before use, and the medium was exchanged with fresh 2% serum. After 120 μL of SEP-1/SiO_2@NH_2 was added to each well plate, all sample cells were incubated for 15 min at 37 °C and then the medium was removed and washed several times with PBS (pH 7.4).

Measurements. ^{1}H NMR spectra (TMS) were recorded on a Bruker UltraShield 500 MHz spectrometer. Elemental analysis (EA) was carried out on a Flash EA1112 from ThermoQuest Italia SPA. FT-IR spectra were recorded on a Bruker IFS66 V FT-IR spectrometer equipped with a DTGS detector (32 scans). Transmission electron microscopy (TEM) images were obtained on a JEOL-2010 electron microscope operating at 200 kV. Luminescence measurements were made on a Hitachi F-4500 fluorescence spectrophotometer. UV−vis spectra were recorded on a Shimadzu 3100 PC spectrometer. The lifetime curves were obtained from a LeCroy Wave Runner 6100 digital osilloscope (1 GHz) using a 290 laser (pulse width = 4 ns, gate = 50 ns) as the

(8) (a) Kim, J.; Lee, J. E.; Lee, J.; Yu, J. H.; Kim, B. C.; An, K.; Hwang, Y.; Shin, C. H.; Park, J. G.; Kim, J.; Hyeon, T. *J. Am. Chem. Soc.* **2006**, *128*, 688–689. (b) Yi, D. K.; Selvan, S. T.; Lee, S. S.; Papaefthymiou, G. C.; Kundaliya, D.; Ying, J. Y. *J. Am. Chem. Soc.* **2005**, *127*, 4990–4991. (c) Yang, Y. H.; Gao, M. Y. *Adv. Mater.* **2005**, *17*, 2354–2357. (d) Zhao, X. J.; Bagwe, R. P.; Tan, W. H. *Adv. Mater.* **2004**, *16*, 173–176.

(9) (a) Green, M.; Harries, J.; Wakefield, G.; Taylor, R. *J. Am. Chem. Soc.* **2005**, *127*, 12812–12813. (b) Chan, Y.; Zimmer, J. P.; Stroh, M.; Steckel, J. S.; Jain, R. K.; Bawendi, M. G. *Adv. Mater.* **2004**, *16*, 2092–2097.

(10) Zheng, L.; Gu, Z. J.; Ma, Y.; Zhang, G. J.; Yao, J. N.; Keita, B.; Nadjo, L. *J. Biol. Inorg. Chem* **2010**, *15*, 1079−1085.

(11) Sugeta, M.; Yamase, T. *Bull. Chem. Soc. Jpn.* **1993**, *66*, 444–449.

(12) Sousa, F. L.; Pillinger, M.; Sá Ferreira, R. A.; Granadeiro, C. M.; Cavaleiro, A. M. V.; Rocha, J.; Carlos, L. D.; Trindade, T.; Nogueira, H. I. S. *Eur. J. Inorg. Chem.* **2006**, 726–734.

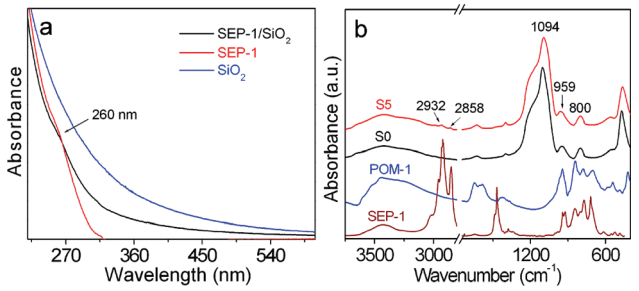

Figure 1. (a) UV−vis spectra of SEP-1, SEP-1/SiO_2 (S4), and pure SiO_2 nanoparticles and (b) IR spectra of POM-1, SEP-1, SEP-1/SiO_2 (S5), and pure SiO_2 (S0) nanoparticles.

excitation source (Continuum Sunlite OPO). Imaging measurements were performed on an FV1000 confocal laser fluorescence microscope (Olympus) with a 10× objective lens. The excitation wavelength for loaded cells was selected to be 330−385 nm. X-ray photoelectron spectroscopy (XPS) measurements were performed on an Escalab Mark (VG) photoelectron spectrometer using a monochromatic Al Kα X-ray source. ζ potentials were used on a Malvern Nano ZS ZEN3600. The inductively coupled plasma optical emission spectrometry (ICP-OES) used to determine the concentration of a wide range of elements in solutions was carried out on a Thermo Scientific iCAP ICP-OES 6000 series.

Results and Discussion

Structural Characterization of SEP-1. The EA and TGA (Supporting Information (SI), Figure S1) measurements of the prepared SEP-1 complex are in agreement with the reported results,[6a] revealing the anticipated chemical composition. The UV−vis spectrum of SEP-1 exhibits the characteristic absorption band of POM-1 at around 260 nm, which can be assigned to the oxygen-to-tungsten ligand-to-metal charge-transfer (O → W LMCT) transition (Figure 1a). The FT-IR spectrum displays the characteristic vibrational modes of both DOHDA and POM-1, as found in each separated component and summarized in the Experimental Section. The corresponding spectral changes are derived from the electrostatic interaction between DOHDA and POM-1 in SEP-1, implying the successful encapsulation of the surfactant on the inorganic cluster (Figure 1b).[13]

Preparation and Morphological and Structural Characterizations of SEP-1/SiO_2 Nanoparticles. Because the hydroxyl group is covalently modified to the hydrophobic terminal group of the alkyl chain, it is expected to be located on the outside surface of SEP-1 after cationic DOHDA covers polyanion POM-1 electrostatically,[6a,13] which makes the complex a bit more hydrophilic. As a result, SEP-1 becomes soluble in the solution of ethanol and water, which is helpful for further reaction with hydrolyzed TEOS, leading to chemical fixation to the network of the silica matrix of nanoparticles and forming SEP-incorporated SiO_2 nanoparticles, as illustrated in Scheme 1.

On the basis of the conditions for the preparation of silica nanoparticles through the sol−gel reaction, weak alkalinity is required and more nucleation seeds are usually favorable to the formation of smaller particles.[14] The obtained SEP-1-grafted silica nanoparticles with different doping contents were well-characterized. From TEM observations (Figure 2), it is distinctly seen that the hybrid particles have a narrow size distribution, good dispersion, and a smooth surface. The size scale of the silica nanoparticles tends to decrease with increasing loading content of SEP-1. Under the same preparation conditions, including the same volume of ethanol, ammonia, and TEOS, the size statistics according to TEM images provides diameters on the order of 48, 42, and 23 nm (Figure S2) for S0 (pure SiO_2 nanoparticle), S4, and S5, respectively. This result implies that SEP-1 complexes bearing hydroxyl groups on the periphery act as seeds to promote the nucleation of primary particles directing to the final hybrid silica nanoparticles.

The UV−vis spectrum of SEP-1/SiO_2 (S4) exhibits the characteristic absorption of SEP-1 at around 260 nm (Figure 1a), which is very close to the O → W LMCT band of pure POM-1.[6] Compared with the pure silica nanoparticle (S0), the IR spectrum (Figure 1b) of hybrid SEP-1/SiO_2 nanoparticles (S5) displays additional vibrations at 2932 and 2858 cm^{-1}, which should be derived from the characteristic ν_{as} (CH_2) and ν_s (CH_2) vibrational modes of DOHDA, respectively. Meanwhile, the bands that should be obtained from ν_{as} (Si−O−Si), ν (Si−O−H), and ν_s (Si−O−Si) appear at around 1094, 959, and 800 cm^{-1}, respectively, indicating the existence of SEP-1 in the silica matrix.[13] Because of bands overlapping with the silica matrix, the vibrational modes of POM-1 could not be recognized distinctly from the IR spectrum. Fortunately, the fluorescence spectra show the characteristic excitation band around 290 nm (LMCT) and emission bands at 578, 593, 612, 650, and 700 nm that are attributed to $^5D_0 \rightarrow {}^7F_j$ (j = 0, 1, 2, 3, 4) of Eu^{3+} transitions, indicating the stability of POM-1 during the preparation of hybrid nanoparticles (Figure 3a).[6]

The successful introduction of SEP-1 into silica nanoparticles can be directly observed from the color changes of samples under UV light irradiation, as shown in Figure 4. With increasing content of SEP-1, the observed luminescent color changes gradually from blue for pure silica nanoparticles (S0)[15] without SEP-1 to purple that combines the luminescence of pure silica particles and POM-1 (S1−2) and finally to red (S3, S6), where the color of the Eu ion becomes dominant.[16] Moreover, the magnified TEM images further confirm the uniform SEP-1 inlay in the silica matrix, as demonstrated in the insets of Figure 2b,c. The darkish spots corresponding to SEP-1 are found to be dispersed uniformly in inner silica nanoparticles.

The ζ-potential measurements reveal similar surface potentials of −49.0, −44.9, and −50.7 mV for S0, S4, and S5 (Figure 5), indicating similar surface properties of SEP-1-grafted silica nanoparticles to those of pure silica nanoparticles, where a surface bearing hydroxyl groups can be concluded. This result also implies that almost all SEP-1 complexes are located inside rather than on the surface of the hybrid nanoparticles. XPS analysis shows a similar surface composition between pure SiO_2 nanoparticles and S4 hybrid nanoparticles, but the XPS spectra of HF-etched S4 nanoparticles obviously show the appearance of W 4f, W $4d_{5/2}$, W $4d_{5/2}$, W $4d_{5/2}$, and W $4d_{5/2}$ at 37, 248, 261, 402, and 428 eV, respectively. The above results indicate that almost all SEP-1 complexes are located inside rather than on the surfaces of hybrid nanoparticles, even in the cases of S5 and S6 in which higher concentrations of the complex were employed (Figure 3b). The chemical grafting of SEP-1 inside the silica matrix can be

(13) (a) Zhao, Y. Y.; Qi, W.; Li, W.; Wu, L. X. *Langmuir* **2010**, *26*, 4437–4442. (b) Qi, W.; Li, H. L.; Wu, L. X. *J. Phys. Chem. B* **2008**, *112*, 8257–8263.

(14) (a) Stöber, W.; Fink, A.; Bohn, E. *J. Colloid Interface Sci.* **1968**, *26*, 62–69. (b) van Blaaderen, A.; van Geest, J.; Vrij, A. *J. Colloid Interface Sci.* **1992**, *154*, 481–501.

(15) (a) Brankova, T.; Bekiari, V.; Lianos, P. *Chem. Mater.* **2003**, *15*, 1855–1859. (b) Carlos, L. D.; Sá Ferreira, R. A.; Pereira, R. N.; Assunção, M.; de Zea Bermudez, V. *J. Phys. Chem. B* **2004**, *108*, 14924–14932.

(16) (a) Yamase, T.; Kobayashi, T.; Sugeta, M.; Naruke, H. *J. Phys. Chem. A* **1997**, *101*, 5046–5053. (b) Carlos, L. D.; Messadeq, Y.; Brito, H. F.; Sa-Ferreira, R. A.; de Zea Bermudz, V.; Ribeiro, S. J. L. *Adv. Mater.* **2000**, *12*, 594–598. (c) Zhang, T. R.; Spitz, C.; Antonietti, M.; Faul, C. F. J. *Chem.−Eur. J.* **2005**, *11*, 1001–1009.

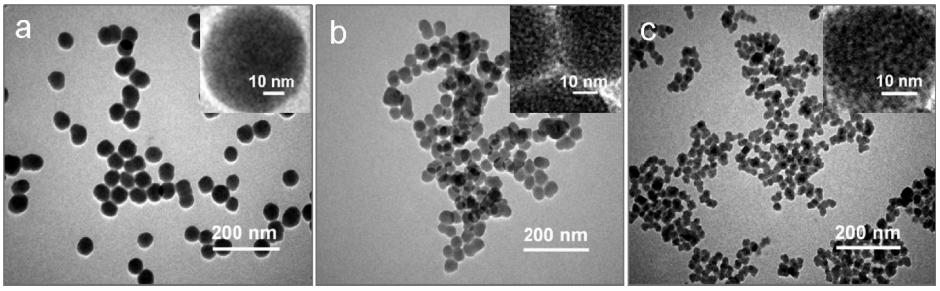

Figure 2. TEM images of (a) S0, (b) S4, and (c) S5 with insets of the corresponding magnified image.

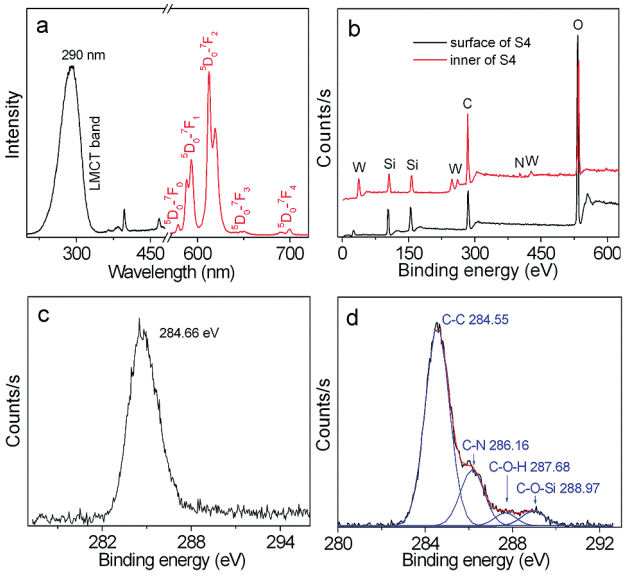

Figure 3. (a) Excitation and emission spectra of S6. XPS spectra of S4 (b) before and after etching with 1% HF solution for a short time and corresponding bands of C 1s binding energy (c) before and (d) after surface etching by HF solution.

further confirmed through the appearance of the C 1s binding energy of the C−O−Si bond at 288.97 eV in the XPS spectrum of HF-etched hybrid silica nanoparticles. Similar to the pure silica nanoparticles, a single band of C binding energy at 284.66 eV is found in the case of S4 (Figure 3c) and other nanoparticles without etching by HF, which is possibly derived from the residual C element left by incompletely hydrolyzed TEOS. In contrast to the spectrum with respect to the surface of silica nanoparticles, those nanoparticles etched with HF display a broad band that can be fit into four separate bands at 284.55, 286.16, 287.68, and 288.97 eV (Figure 3d), which can be assigned to all C element binding possibilities, C−C, C−N, C−O−H, and C−O−Si bonds in turn.[13] The estimated peak area ratio of C−C, C−N, and C−O (including C−O−Si and C−OH) is ca. 8:2:1, which is approximately coincident with the corresponding C atom ratio of 9:2:1 calculated from the molecular formula of DOHDA. On the basis of the peak area ratio of 0.8:1 between C−O−H and C−O−Si, we assume that more than 56% of C−OH in SEP-1 is chemically grafted into the silica matrix through the formation of the C−O−Si bond.[13] Therefore, both the XPS and TEM results indicate that POM-1 was successfully incorporated into silica nanoparticles through the covalent bonding of hydroxyls on the surface of SEP-1 and uniform inlays inside the silica matrix.

To identify the consistency of the SEP-1 concentration in the reaction system with that incorporated in the hybrid silica nanoparticles, the supernatant of the sol−gel reaction solution of hybrid S4 was collected and analyzed by ICP measurements. The measured results of Si in 58.04 and W in 18.74 μg/mL indicate that over 99.9 wt % of TEOS and 99.5 wt % of SEP-1 were transferred to the obtained hybrid nanoparticles. Therefore, we believe that the SEP-1 complex has been grafted into hybrid nanoparticles almost quantifiably. Such a result is reasonable because of the good miscibility of SEP-1 as the nucleating seed with the TEOS solution. The reaction process can be understood as occurring when the SEP-1 complexes react with hydrolyzed TEOS, forming primary nuclei and subsequently growing into hybrid silica nanoparticles.

Photophysical Properties of SEP-1/SiO_2 Nanoparticles. Because the Eu-substituted POM was employed in the present study, the photophysical properties of the prepared SEP-1/SiO_2 nanoparticles should mainly originate from the rare earth ion. It is widely accepted that the $^5D_0 \rightarrow {}^7F_2$ transition is an electronic dipole transition, which is sensitive to the local chemical environment of Eu^{3+}, whereas the $^5D_0 \rightarrow {}^7F_1$ transition is a magnetic dipole transition and its intensity is insensitive to the microenvironment of Eu^{3+}. This property was used as a reference to calculate the absolute emission quantum yields (η) of POM-1, SEP-1, and the hybrid nanoparticle.[6,11] The excitation and emission spectra of S1, S2, S3, and S6 can be seen in the SI (Figures S3−S6). On the basis of the band intensity changes of Eu^{3+} in the emission spectra, we determined the integral intensity ratio of $^5D_0 \rightarrow {}^7F_j$ (j=0, 1, 2, 3, 4) to $^5D_0 \rightarrow {}^7F_1$ transitions. The total radiative rate (k_r) of $^5D_0$ can be calculated from eq 1[11,16]

$$k_r = k_{r(0\rightarrow 1)} \frac{\sum_{j=0}^{4} S_{(0\rightarrow j)}}{S_{(0\rightarrow 1)}} \quad (1)$$

where $k_{r(0\rightarrow1)}$ is the characteristic radiative rate of the $^5D_0 \rightarrow {}^7F_1$ transition with a reported value of 1.35×10^2 s^{-1}.[11,16a] The $^5D_0$ decay curves of pure SEP-1 and hybrid nanoparticles can be well fitted to a single-exponential function. The fitted lifetimes (in milliseconds) are shown in Table 1. From these data, the total decay rate of $^5D_0$ (k_{tot}) can be calculated from eq 2

$$k_{tot} = \frac{1}{\tau} = k_r + k_{nr} \quad (2)$$

where k_{nr} is the nonradiative rate. Finally, the quantum yield can be estimated from eq 3

$$\eta = \frac{k_r}{k_r + k_{nr}} \quad (3)$$

The photophysical data of Eu^{3+} in different environments (POM-1, SEP-1, and hybrid nanoparticles), calculated from the emission spectra and the lifetime, are summarized in Table 1.

In comparison to that of POM-1, the lifetime of the SEP-1 complex becomes shorter, indicating a decrease in the number of

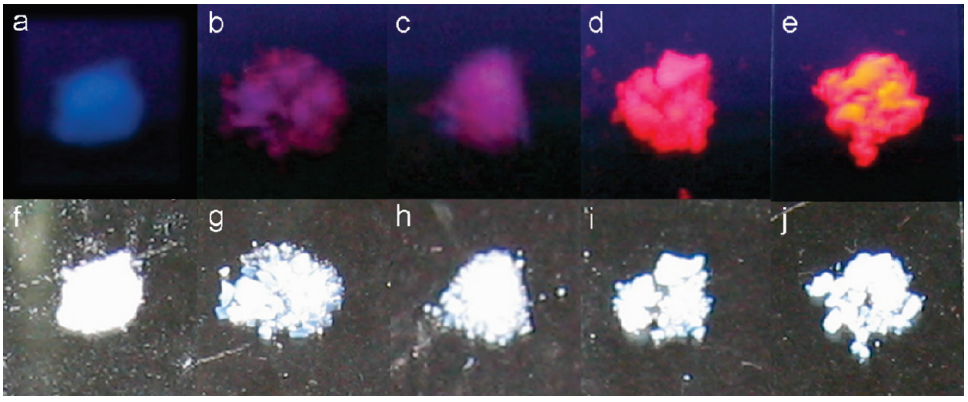

Figure 4. Digital photographs of (a) S0, (b) S1, (c) S2, (d) S3, and (e) S6 under UV irradiation of 254 nm light at a distance of 25 cm and corresponding photographs of (f−j) these samples taken under room light, respectively.

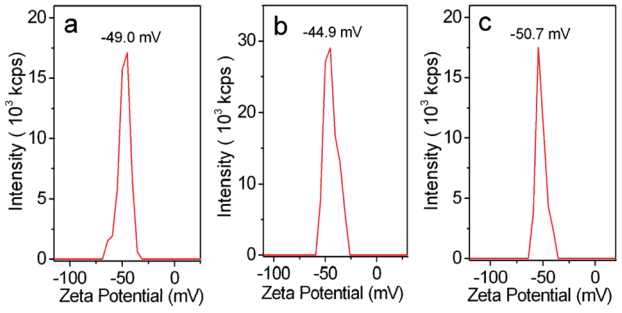

Figure 5. ζ-potential plots of (a) S0, (b) S4, and (c) S5 in aqueous solution.

Table 1. Summary of the Photophysical Data of Eu^{3+} in POM-1, SEP-1, and SEP-1/SiO_2 Nanoparticles (S1, S2, S3, and S6)

sample	LMCT (nm)	$I_{(0\rightarrow2)}/I_{(0\rightarrow1)}$	$S_{(0\rightarrow1)}/\Sigma S_{(0\rightarrow j)}$	t (ms)	k_{tot} (ms^{-1})	k_r (ms^{-1})	k_{nr} (ms^{-1})	η (%)
POM-1 (solid)	278	0.16	0.37	2.80	0.38	0.27	0.09	75.62
SEP-1 (solid)	261	0.97	0.44	1.82	0.55	0.31	0.24	56.37
S1 (solid)	285	3.66	0.17	0.83	1.20	0.86	0.34	71.67
S2 (solid)	285	3.02	0.17	0.87	1.15	0.77	0.38	66.96
S3 (solid)	285	2.39	0.14	0.93	1.08	0.48	0.60	44.44
S6 (solid)	290	2.56	0.13	1.23	0.81	0.52	0.29	64.20

coordinated water molecules on the Eu ion as a result of the encapsulation and phase-transfer process, which is in agreement with the reported results.[17] Interestingly, the lifetimes of the europium ion, accompanied by the covalent incorporation of SEP-1 into the silica matrix, show an increasing tendency with increasing doping concentration. As seen in Table 1, the quantum yield decreased in some extent after the surface modification of Eu^{3+}-substituted POM due to the change in the surface chemical microenvironment. However, the quantum yields of the SEP complex in SiO_2 particles did not decrease continuously because of the protection of hydrophobic encapsulation. Although the decrease in the luminescence intensity was surely unfavorable to detection in the labeling experiment, it still falls into the acceptable range because we could observe the luminescence around the labeled cells, as revealed in the following part of this article. These results suggest that the structure and luminescence of POM-1 are retained in both SEP-1 and hybrid nanoparticles, and the hybrid nanomaterials have a high luminescence quantum yield and could

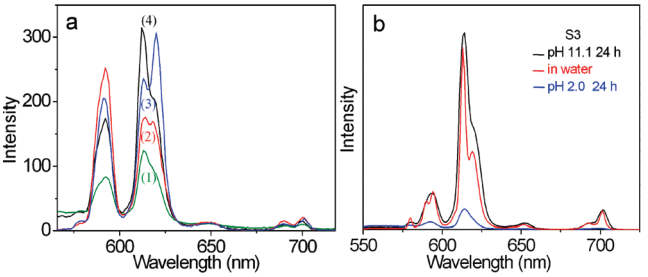

Figure 6. (a) Emission spectra of SEP-1 (0.32 mg/mL) under the same concentration as used in the preparation of S4 in the solution for the sol−gel reaction after (1) 30 h and (2) 10 min and (3) in ethanol and (4) SEP-1/SiO_2 (S4) in the solution for the sol−gel reaction for 24 h, with excitation at 265 nm. (b) Emission spectra of S3 in aqueous solutions at pH 11.1, 7.0, and 2.0 with excitation at 275 nm.

be applied as potential fluorescence probes. Apparently, the well-maintained luminescence properties in hybrid nanoparticles should be derived from the protection of the DOHDA layer because of its hydrophobic effect in water solutions.[6a,18]

Luminescence Stability of SEP-1/SiO_2 Nanoparticles. To examine the luminescence stability of the prepared SEP-1-grafted SiO_2 nanoparticles, a 94% ethanol solution at pH 10.9, adjusted with ammonia, was employed. In comparison to the case in pure ethanol, the luminescence intensity of SEP-1 decreases visibly in the alkaline aqueous/ethanol solution and when lasting for a longer time (e.g., 30 h) (Figure 6a). In contrast, under the same POM-1 concentration, SEP-1/SiO_2 nanoparticles in the alkaline solution maintain their luminescence quite stably, close to the luminescence intensity of SEP-1 in pure ethanol even after 24 h, indicating the high luminescence stability due to the immobilization of SEP-1 in the silica matrix. Although the luminescence intensity of SEP-1/SiO_2 nanoparticles decreases sharply at pH 2 (Figure 6b), it is still far stronger than that of pure POM-1 at the same pH. Meanwhile, in contrast to the stabilized pH 5.5−8.5 for POM-1,[19] the pH range for SEP-1/SiO_2 nanoparticles with stable luminescence extends to 2−11, which is favorable for functional application under various conditions. Therefore, the replacement of original counterions of POM-1 with −OH-terminated long-alkyl-chain surfactant ensures the successful preparation of hybrid SEP-1/SiO_2. The effect can definitely be ascribed to the

(17) Ballardini, R.; Mulazzani, Q. G.; Venturi, M.; Bolletta, F.; Balzani, V. *Inorg. Chem.* **1984**, *23*, 300–305.

(18) Li, H. L.; Li, P.; Yang, Y.; Qi, W.; Sun, H.; Wu, L. X. *Macromol. Rapid Commun.* **2008**, *29*, 431–436.

(19) Kim, H. S.; Hoa, D. T. M.; Lee, B. J.; Park, D. H.; Kwon, Y. S. *Curr. Appl. Phys.* **2006**, *6*, 601–604.

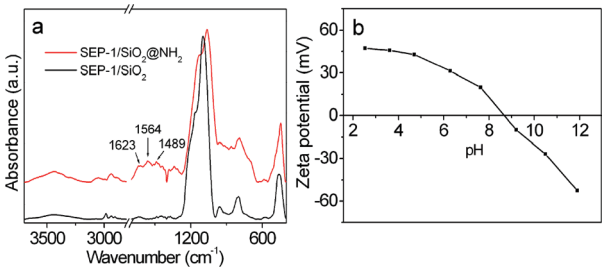

Figure 7. (a) IR spectra of SEP-1/SiO_2 (S6) and its surface-modified SEP-1/SiO_2@NH_2 nanoparticles. (b) Plot of the ζ potential of SEP-1/SiO_2@NH_2 vs the pH change in aqueous solution.

protection of hydrophobic alkyl chains around each POM-1 and the immobilization of SEP-1 in the silica matrix through covalent condensation. Also, this kind of protection and fixation cause POM-1 in the hybrid nanomaterials to display lasting stability. Figures S3−S6 illustrate the luminescence stability of SEP-1/SiO_2 nanoparticles after being aged for 18 months.

Considering the possible leakage due to ion exchange in electrolyte solution, we evaluate the stability of the hybrid nanoparticles soaked in a 0.4 M NaCl solution for 1 week. The examination of the soaked solution indicates that no obvious release of POM-1 from silica nanoparticles as a result of the possible ion exchange between the added salt and SEP-1 complex was found. In addition, because of the multiple covalent bondings of SEP-1 to the silica matrix, it is almost impossible for a whole SEP-1 to disassociate from the silica matrix. Therefore, both the hydrophobic protection and an average micropore size of less than ca. 0.75 nm for the silica matrix block the ion-exchange-induced leakage of POM-1 from silica nanoparticles. This advantage implies the possibility of the POM-incorporated silica nanoparticle serving as a luminescent probe for living cells.

SEP-1/SiO_2@NH_2 Preparation and Fluorescence Labeling of Hela Cells. To incorporate the SEP-1/SiO_2 nanoparticles into living cells more conveniently, the surfaces of the nanoparticles were modified with amino groups, as normally used in the literature.[20] The APS-modified hybrid SiO_2 nanoparticles were characterized by their IR spectrum, EA, and ζ potential. The vibration appearing at 1564 cm^{-1} should correspond to an NH_2 scissor vibration, the vibration at 1489 cm^{-1} can be attributed to the symmetric $-NH_3^+$ deformation mode, and the vibration at 1622 cm^{-1} can be assigned to the asymmetric $-NH_3^+$ deformation mode, whereas the band at 3300 cm^{-1} can be ascribed to the N−H stretching vibration. These vibrations indicate the successful surface modification of APS on the nanoparticles (Figure 7a).[21] EA with respect to the content of the N element in SEP-1/SiO_2@NH_2 increasing from 0.1 to 3.85 wt % (Table S1) support the introduction of APS onto the surface of SEP-1/SiO_2 hybrid nanoparticles. Meanwhile, in comparison to the isoelectric point (iep) of hybrid SEP-1/SiO_2 nanoparticles at around pH 2.0, this value for the resulting SEP-1/SiO_2@NH_2 nanomaterials moves to pH 8.7 (Figure 7b), indicating that the Si−OH surface groups have been partially replaced by $-NH_2$.

To demonstrate the performance of SEP-1/SiO_2@NH_2 nanoparticles, we chose Hela cells as the target bio-objects. The living cells were incubated with APS-modified SEP-1/SiO_2 nanoparticles for 15 min at 37 °C.[22] The luminescence pattern of the labeled

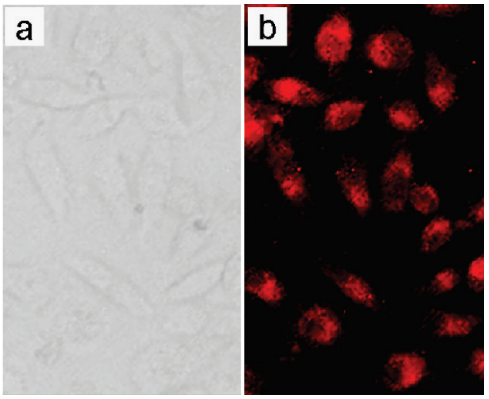

Figure 8. Luminescent optical micrographs of SEP-1/SiO_2@NH_2-labeled Hela cells incubated with SEP-1/SiO_2@NH_2 for 15 min and washed several times with PBS under (a) a bright field and (b) a dark field with UV irradiation at 254 nm.

living cells was clearly observed under the excitation of 254 nm light. The rough shape of the cells can be seen from the bright-field optical microscopy photograph through adjusting the contrast, as shown in Figure 8a. In contrast, through laser confocal fluorescence microscopy observation under the shortest-wavelength excitation of 330−385 nm, we can clearly see the living cells, indicating the dying effect of the nanoparticles. However, the observed living cells in blue should be attributed to the emission of silica nanoparticles themselves,[15] rather than the luminescence of the incorporated SEP-1 complex due to the difference in excitation wavelength. When a substituted 254 nm excitation was applied, red-color-labeled living cells could be clearly found (Figure 8b). For convenience in excitation, most of the luminescent dyeing agents are selected and excited with visible light. The present result provides an additional possibility for cell observation with multiple colorations because the present coloration approach is easy to separate from the normal dyeing domain in the cells only through changing the excitation wavelength.

Conclusions

We successfully developed an approach to prepare luminescent hybrid silica nanoparticles through using a rare earth metal ion substituted POM. The surface encapsulation of a hydroxyl-group-terminated double-chain quaternary ammonium cation through ionic substitution protects the structure and photophysical properties of the incoporated POM under alkaline reaction conditions through forming a hydrophobic layer. The electrostatic interaction between the organic ammonium ion and POM and the covalent interaction between the −OH terminal group and the silica matrix ensure the luminescence stability and avoid the leakage of POM. Importantly, the luminescence of POM incorporated into a silica matrix makes the hybrid nanoparticles a potential luminescent coloration agent. The surface amino-modified hybrid nanoparticles can obviously dye the living Hela cells, allowing them to be observed conveniently through a confocal microscope. Because the luminescence of Eu ions requires excitation at short wavelengths, the hybrid nanoparticle can be used as a special dyeing agent separate from others, which are normally excited with visible light.

Acknowledgment. This work was financially supported by the National Basic Research Program of China (2007CB808003), the National Natural Science Foundation of China (20703019,

(20) Tan, M. Q.; Wang, G. L.; Hai, X. D.; Ye, Z. Q.; Yuan, J. L. *J. Mater. Chem.* **2004**, *14*, 2896–2901.
(21) Pasternack, R. M.; Amy, S. R.; Chabal, Y. J. *Langmuir* **2008**, *24*, 12963–12971.
(22) Li, H. W.; Li, Y.; Dang, Y. Q.; Ma, L. J.; Wu, Y. Q.; Hou, G. F.; Wu, L. X. *Chem. Commun.* **2009**, 4453–4455.

20731160002, 20973082, and 50973042), and an open project of the State Key Laboratory of Polymer Physics and Chemistry of CAS.

Supporting Information Available: TGA curve of SEP-1. Statistical particle sizes of S0, S4, and S5 from TEM graphs. The fluorescence of S1, S2, S3, S6, and SEP-1/SiO_2@NH_2. EA data of SEP-1/SiO_2 (S6) and SEP-1/SiO_2@NH_2 and digital photographs of Hela cells under natural light and UV irradiation, with and without the incubation of SEP-1/SiO_2@NH_2 nanoparticles. This material is available free of charge via the Internet at http://pubs.acs.org.